

**NUMERICAL SIMULATION OF MECHANICAL CONTACT PROBLEMS
USING THE RKPM WITH LOWER INTEGRATION SCHEME**

**Kalilou SIDIBE^{1*}, Guangyao LI², Amadou OUANE³ and
Hamadoun BOKAR⁴**

¹*DER Génie Industriel, Ecole Nationale d'Ingénieurs – Abderhamane Baba
Touré (ENI-ABT), BP 242, Bamako, Mali*

²*College of Mechanical and Automotive Engineering, Hunan University,
410082 Changsha, P.R. China; gyli@hnu.cn*

³*DER Génie Industriel, ENI – ABT, BP 242, Bamako, Mali*

⁴*DER Géologie, ENI – ABT, BP 242, Bamako, Mali*

(Reçu le 16 Mars 2009, accepté le 03 Juillet 2009)

* Correspondance et tirés à part, e-mail : kalsidibe@yahoo.fr

ABSTRACT

A simple contact algorithm based on the penalty approach is implemented in a two-dimensional Reproducing Kernel Particle Method (RKPM) to simulate mechanical contact involving large deformation of mechanical structures. In order to reduce the computing time a lower integration scheme, two-point quadrature for quadrilateral background mesh, is used. The standard Taylor bar impact problem simulation is used to validate the results obtained using the presented contact algorithm by comparing with those obtained using the commercial Finite Element Analysis code LS-DYNA3D; an excellent agreement is obtained.

Keywords : *RKPM, lower integration, mechanical contact, deformation.*

RÉSUMÉ

Simulation numérique des problèmes de contact mécanique en utilisant la RKPM avec une méthode d'intégration réduite

Un algorithme simple, basé sur l'approche pénalité, est implémenté dans la RKPM (Reproducing Kernel Particle Method) à 2D pour simuler les problèmes de contact mécanique produisant de large déformation. Pour réduire, de façon significative, le temps de calcul une méthode d'intégration, à deux-points dans les cellules d'intégration du maillage d'arrière plan, est utilisée. Le problème standard de simulation de l'impact de la barre de Taylor

est utilisé pour valider les résultats obtenus par l'algorithme présenté en les comparant à ceux obtenus par l'utilisation du logiciel commercial d'Analyse des Eléments Finis LS-DYNA3D ; une excellente concordance est obtenue.

Mots-clés : *RKPM, intégration réduite, contact mécanique, déformation.*

I - INTRODUCTION

In computational mechanics, the simulation of large deformation of mechanical structures has been a challenging task. Significant amount of work has been accomplished using the finite element methods. Nevertheless, standard finite element approaches are still ineffective in handling extreme material distortions. To overcome such difficulties, considerable effort has been devoted to the development of meshless or meshfree methods. Among the meshless methods, the reproducing kernel particle method (RKPM) [1-7], has been found to be very effective for large deformation analysis as encountered in metal forming [2, 6-8].

Like the others meshless methods, the RKPM is characterized by its high CPU cost. In our implementation of RKPM the background mesh is currently used for integration purposes. The integration of the stresses for the calculation of internal forces involves several loops over the gauss quadrature points. Therefore reducing the number of gauss quadrature points, without affecting the accuracy of the results, will improve significantly the computation efficiency. In this work, the two gauss quadrature points rule, developed by K. SIDIBE et al. [5], is used and compared with the traditional 2×2 gauss rules.

Also, the simulation of the mechanical contact is a challenging task [6-9]. In this work, a simple contact algorithm "particle to segment contact algorithm" for two-dimensional RKPM is developed and implemented in our RKPM code. The standard Taylor bar impact problem simulation is used to prove the correctness of the algorithm and its implementation in our RKPM code comparing the results with those obtained by using the commercial Finite Element Analysis code LS-DYNA3D.

II - FUNDAMENTAL CONCEPTS

II-1. RKPM discretization

The RKPM has been found to be very effective for large deformation analysis [2]. This work focuses on the 2D RKPM computer implementation issues.

The RKPM uses the finite integral representation of a function $u(\mathbf{x})$ in a domain Ω_x .

$$u^a(\mathbf{x}) = \int_{\Omega_x} \Phi_a(\mathbf{x} - \mathbf{y})u(\mathbf{y})d\Omega_x \tag{1}$$

where $u^a(\mathbf{x})$ is the approximation of function $u(\mathbf{x})$, $\Phi_a(\mathbf{x} - \mathbf{y})$ is the kernel function with compact support a [1].

Discretizing the domain Ω_x by a set of particles $\{\mathbf{x}_1, \mathbf{x}_2, \dots, \mathbf{x}_{NP}\}$, where \mathbf{x}_I is the position vector of particle I , and NP is the total number of particles, the integral is approximated by the following summation:

$$u^h(\mathbf{x}) = \sum_{I=1}^{NP} N_I(\mathbf{x})u(\mathbf{x}_I) \tag{2}$$

where $N_I(\mathbf{x})$ is the RKPM shape function defined to be

$$N_I(\mathbf{x}) = C(\mathbf{x}; \mathbf{x} - \mathbf{x}_I)\Phi_a(\mathbf{x} - \mathbf{x}_I)\Delta V_I \tag{3}$$

$C(\mathbf{x}; \mathbf{x} - \mathbf{x}_I)$ is the correction function introduced to improve the accuracy of the approximation near the boundaries and ΔV_I is the volume of particle I and the subscript h is associated with a discretized domain.

II-2. Lower integration rule

The integration of the stresses for the calculation of internal forces involves several loops over the gauss quadrature points so high CPU cost. Therefore to reduce the CPU, instead of the traditional 2×2 gauss rules (called here Q4); K. SIDIBE et al. [5] introduce and validate a lower integration rule in which two gauss quadrature points are set in the integration cell as shown in **Figure I-c**. Applications of this integration method are done for metal forming analysis in this paper.

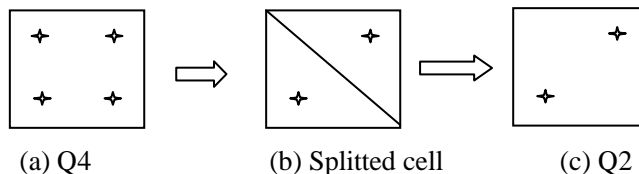


Figure 1 : *Quadrilateral cell with Gauss quadrature points*

II-3. Particle to segment contact algorithm in 2D RKPM

Consider a system of two bodies arbitrarily designated by slave body and master body. The master surface is discretized by a set of master particles connected into piecewise linear segments, and the slave surface by a set of slave particles. Every time step, the algorithm first must predict the accelerations, velocities, and displacements from explicit time integration routine. The resulting displacements are then used to determine whether or not contact has taken place.

The algorithm assumes that slave particles can be penetrating the master surface as shown in *Figure 2*. \mathbf{x}_m and \mathbf{x}_s stand respectively for the spatial coordinates of master and slave particles; while \mathbf{n}_I and \mathbf{t}_I are the normal and the tangential unit vectors of the master segment I .

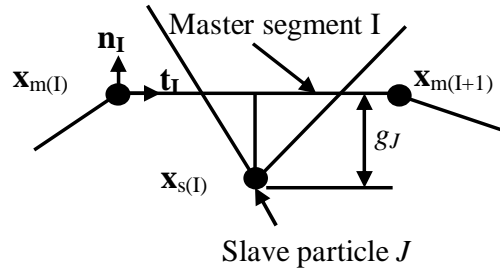


Figure 2 : Discrete contact surfaces

To ensure that the two surfaces do not interpenetrate, the contact force applied to the penetrating slave particle to cancel its normal penetration g_J is calculated as follows:

$$\mathbf{f}_n(J) = \frac{m_s(J) \times g_J}{\Delta t^2} \mathbf{n}_I = f_n(J) \mathbf{n}_I \quad (4)$$

where Δt is the time step size, and $m_s(J)$ is the mass of the slave particle J . On the tangential direction of the contact surface, the classical Coulomb friction model is adopted in modeling friction between slave body and master body. The tangential force exerted by the master surface on a slave particle J is evaluated as

$$\mathbf{f}_{f(J)} = -\min(\mu_k f_{n(J)}, \|\mathbf{f}_{t(J)}^{st}\|) \frac{\mathbf{v}_{TR}(J)}{\|\mathbf{v}_{TR}(J)\|} \quad (5)$$

where μ_k friction coefficient on the contact interface and

$$\mathbf{f}_{t(J)}^{st} = -\frac{\mathbf{m}_s(J)}{\Delta t} \mathbf{v}_{TR}(J) \quad (6)$$

where $\mathbf{v}_{TR}(J)$ is the tangential component of the relative velocity of the slave particle J with respect to the associated master segment.

The force vectors calculated above are the exact nodal force vectors for each penetrating particle to satisfy the impenetrability condition and friction condition at interface. With RKPM the exact nodal force is redistributed to a non-local ‘fictitious force’. The fictitious force vector for the particle I is calculated as follows:

$$\bar{\mathbf{f}}_I = \sum \mathbf{f}_J \mathbf{N}_I(\mathbf{x}_J) \quad (7)$$

The **contact subroutine** called by the main program for contact problem can be outlined as follows:

- i. Find the penetrated slave particles; generate an array containing slave particles penetrations, information about penetrated slave particles and the corresponding master segment;
- ii. Compute normal and frictional forces and redistribute them to the particles;
- iii. Calculate the incremental acceleration due to contact interactions;
- iv. Update velocities and displacements taking into account the contact interactions;
- v. Return to the main program.

III – RESULTS AND DISCUSSION

The simulation of Taylor bar impact and the metal forging will be presented in this section. The elasto-plastic material model with isotropic strain hardening is used for the material modelization in all the examples.

III-1. Taylor bar impact

A cylindrical bar impacts a rigid surface. The data of the problem and the material parameters are defined in *Tables 1* and *2* respectively. Since the problem is axially symmetric, axisymmetric formulation of the governing equations is used and only half of the cylinder is discretized as shown in

Figure 3. The results are compared with the solution obtained using the commercial code LS-DYNA3D.

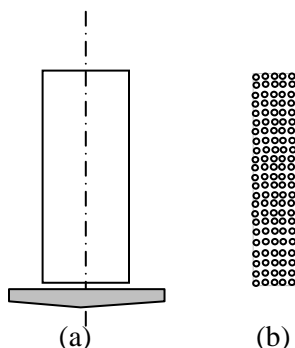


Figure 3 : Taylor bar impact:(a) Continuum domain(b) Discretized domain

At the end of the simulation ($t=80\mu s$) the results obtained by RKPM and LS-DYNA3D are shown in **Table 3** and the corresponding shapes of the bar at the contact surface are shown in **Figure 4**. The time histories of the radius and the height of the bar are shown respectively in **Figure 5** and **Figure 6**. Almost the same results are drawn by RKPM Q2, RKPM Q4 and LS-DYNA3D.

Table 1 : Data of the Taylor bar impact problem

Parameter	Initial velocity	Simulation time	Initial radius	Initial height	Number of particles	Time step size	Friction coefficient
Value	227.0m/s	80 μs	0.0032m	0.0324m	1071 (21 \times 51)	5 $\times 10^{-9}s$	0.0

Table 2 : Material parameters of the bar

Parameter	Young's modulus	Poisson's ration	Initial yield stress	Hardening modulus	Mass density
value	117Gpa	0.35	400Mpa	100Mpa	8930kg/m ³

Table 3 : Comparison of the radius and the height of the bar by various methods at the end of the simulation ($t=80\mu s$)

Solution Methods	Radius	Height
RKPM Q2	7.11 mm	21.59mm
RKPM Q4	7.06 mm	21.58 mm
LS-DYNA3D	7.06 mm	21.52 mm

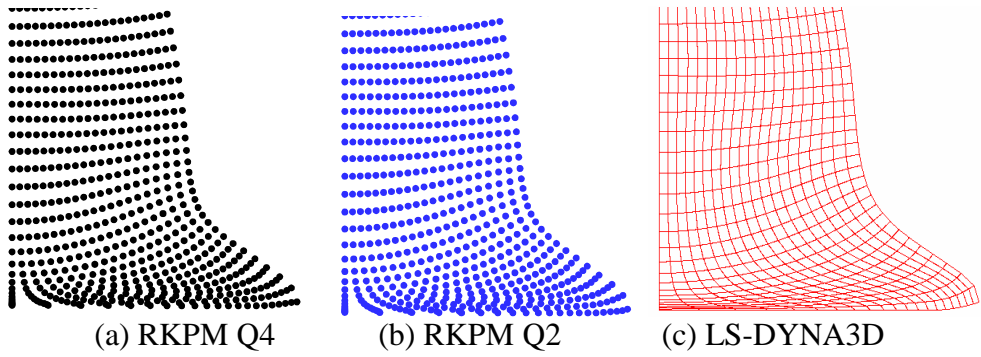


Figure 4 : *Impact of Taylor bar: deformed shape of the bar at the end of the simulation by various methods*

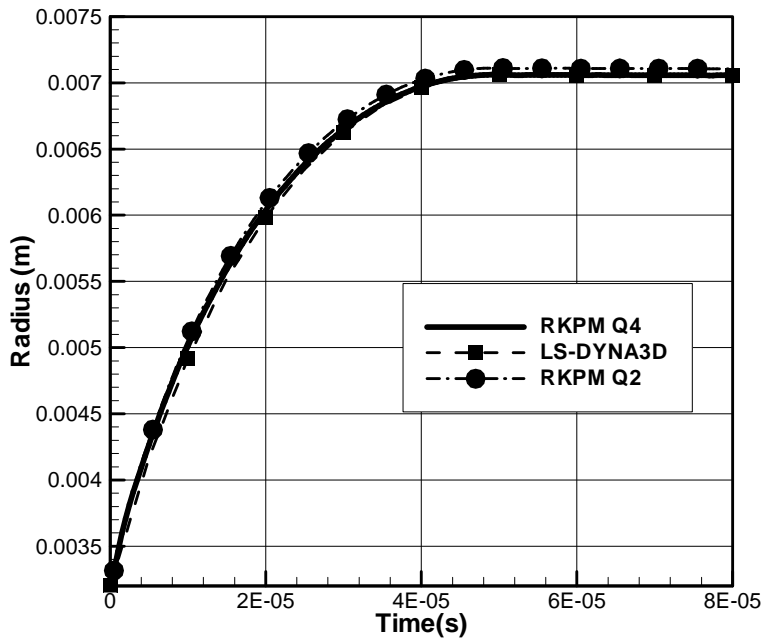


Figure 5 : *Impact of Taylor bar: Time histories of the radius of the bar*

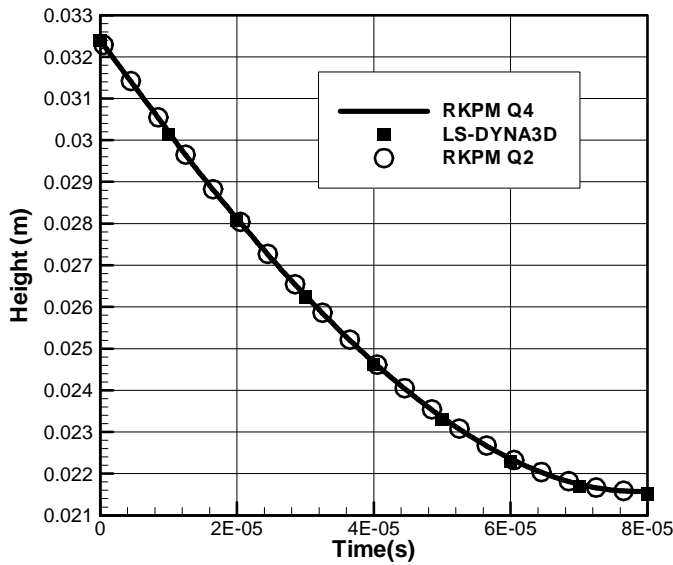


Figure 6 : Impact of Taylor bar: Time histories of the height of the bar

III-2. Square block forging

The plane strain forging by rigid flat tools is considered in this example. A square block of 500mm×500mm is compressed by two rigid flat tools moving in opposite direction with constant velocity of 10m/s. The simulation time is 0.015s. The statement of the problem is shown in *Figure 7*. The friction coefficient is chosen to be $\mu=0.2$. The material properties of the workpiece, discretized by a set of 441 (21×21) particles, are defined in *Table 2*. The evolution of the forging process is shown in *Figure 8*.

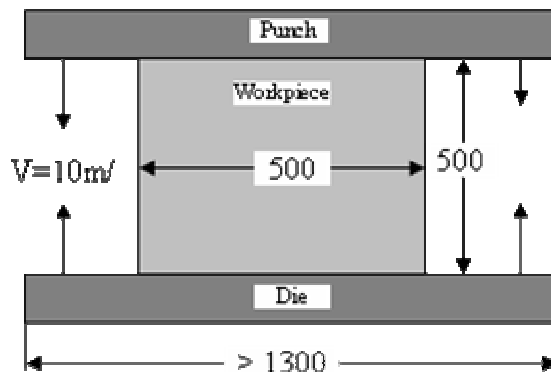


Figure 7 : Statement of the plane strain forging problem

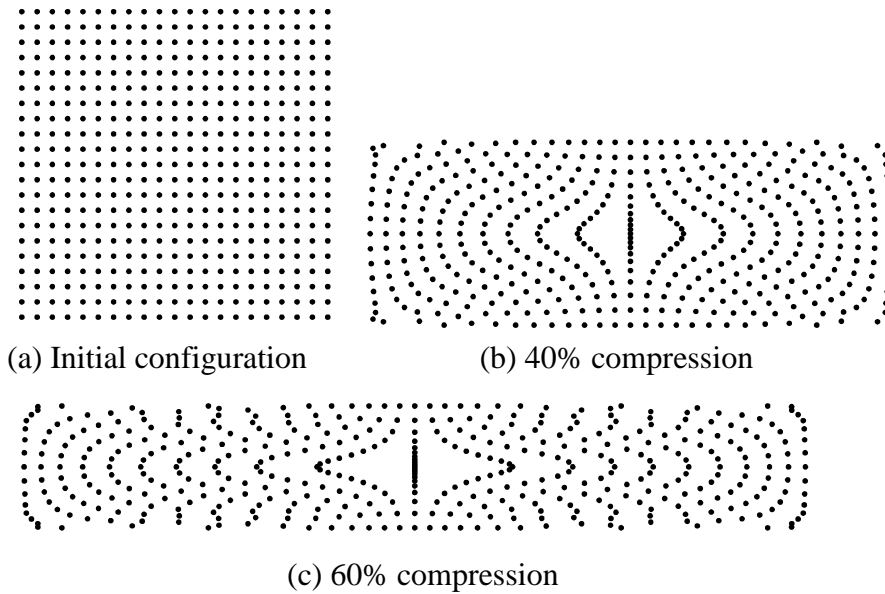


Figure 8 : *Plane strain forging process*

III-3. Wheel forging

This example aims to simulate the cold forging process of a wheel. As shown in **Figure 9-b**, a cylindrical slug is used to obtain a wheel drawn in **Figure 9-a**. The material parameters used for the simulation are given in **Table 4**. Because of the symmetry of the problem an axisymmetric formulation is used and only half of the domain is discretized with 961(30×30) particles. The punch and the die, assumed to be rigid and frictionless, are discretized by piecewise linear segments to fit the geometry of the wheel. The punch is moving downward with constant velocity of 10m/s while the die is fixed. The maximum stroke of the punch at the end of the simulation is 20mm.

Table 4 : *Material parameters of the wheel*

Mass density	Young's modulus	Poisson's ratio	Stress-strain curve
$\rho = 2700 \text{ kg/m}^3$	$E = 71 \text{ GPa}$	$\nu = 0.3$	$\sigma = 576.79(0.01658 + \epsilon_p)^{0.3593} \text{ MPa}$

The finale stages of the deformation are shown in **Figure 9- d and e**; similar results are obtained using RKPM Q4 and RKPM Q2.

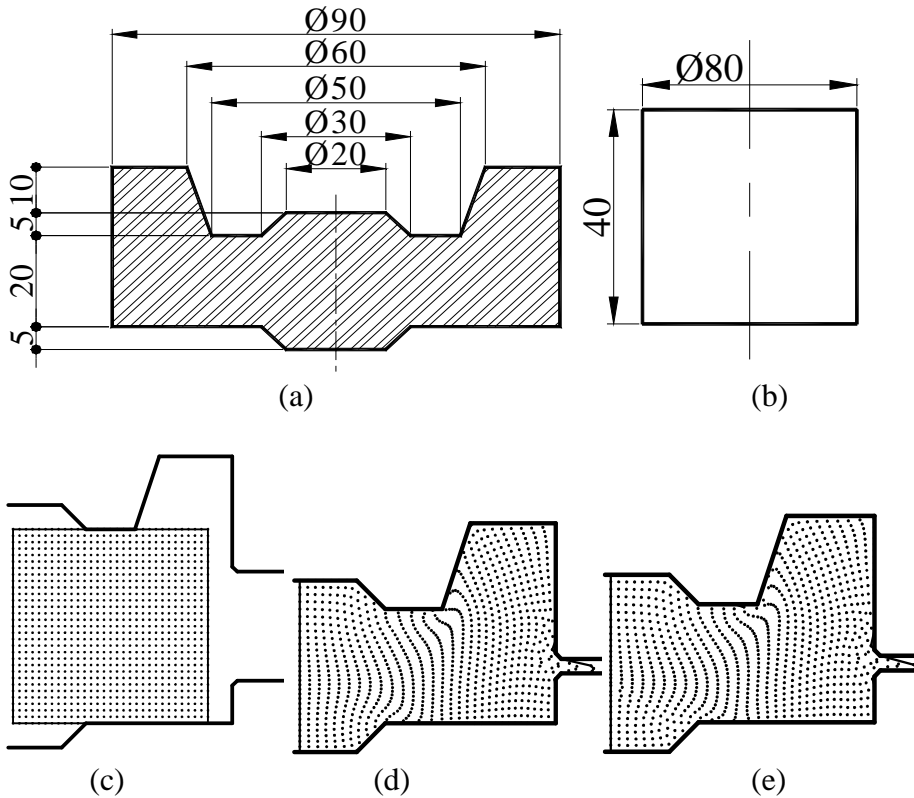


Figure 9 : Cold forging simulation, statement and deformation process by different integration schemes in RKPM:

- (a) Raw slug, (b) Geometry of the wheel, (c) Initial configuration
 (d) Final stage RKPM Q4, (e) Final stage RKPM Q2,

III-4. Comparison of the CPU times

For the three numerical examples, **Table 5** shows the CPU times using the two integration methods. The computation was done using a Pentium (R) 4 CPU – 3.20GHZ with RAM 512Mo. The difference in the percentages of reduction of the CPU time, by the Q2 scheme with respect to the Q4 scheme for these examples, is mostly due to the time consumed by the contact searching algorithm. It is seen that important reduction of the CPU time is obtained by using Q2 scheme.

Table 5 : Comparison of CPU Time

Numerical Examples	Integration Scheme	CPU time	Reduction of CPU time
Taylor bar impact	Q4	20mn38s	47.98%
	Q2	10mn44s	
Block forging	Q4	22mn00s	46.89%
	Q2	11mn41s	
Wheel forging	Q4	25mn09s	47.91%
	Q2	13mn06s	

IV - CONCLUSION

The correctness of the computer implementation of the particle to segment contact algorithm has been shown through numerical examples, the Taylor bar impact and cold forging simulations. The Q2 integration scheme has been also found very efficient for faster computation with almost the same accuracy as the Q4. The effectiveness of the RKPM for large deformations simulation is confirmed.

REFERENCES

- [1] - W. K. LIU, S. JUN and Y. F. ZHANG ‘Reproducing Kernel Particle Methods’ *Int j. Numer. Meth. Fluids*. 20 (1995) 1081-1106
- [2] - S. JUN, W.K. LIU and T. BELYTSCHKO ‘Explicit reproducing kernel particle methods for large deformation problems’ *Int. J. Numer. Meth. Engng.*, 41 (1998) 137-166
- [3] - T. BELYTSCHKO, Y. KRONGAUZ, D. ORGAN, M. FLEMING, and P. KRYSL ‘Meshless Methods: An Overview and Recent Developments’ *structures’ comput Methods Appl.Mech. Engrg, special issue on Meshless Methods* 139 (1996) 3-47,
- [4] - G. R. LIU ‘Mesh-Free Methods, Moving beyond the Finite Element Method’, CRC Press (2002)
- [5] - K. SIDIBE, G.Y. LI, A. OUANE & T. SANOGO ‘Lower Integration Rule and Benchmark Test Procedure for 2D Meshfree Methods’. *Journal Africain de Communication Scientifique* N°7 (2009) 963-968
- [6] - G. Y. LI, K. SIDIBE & G. R. LIU ‘Meshfree method for 3D bulk forming analysis with lower order integration scheme’. *Engineering Analysis with Boundary Elements*, Vol 28 (2004) 1283-1292

- [7] - J. S. CHEN, C. PAN, C. T. WU, W. K. LIU, ‘reproducing kernel particle methods for large deformation analysis of non-linear structures’ *comput Methods Appl. Mech. Engrg* 139 (1996) 195-227
- [8] - J. S. CHEN, H. P. WANG, ‘New boundary condition treatments in meshfree computation of contact problems’ *Comput. Methods Appl. Mech. Engrg.* 187 (2000) 441-468,
- [9] - Z. H. ZHONG ‘Finite Element Procedures for Contact-Impact’, Ed. Oxford University Press (1993)